Comparison between a numerical model and an experimental approach of preform infrared radiative heating-recent results

S Monteix, Fabrice Schmidt, Yannick Le Maoult, G Denis, M Vigny

COMPARISON BETWEEN A NUMERICAL MODEL AND AN EXPERIMENTAL APPROACH OF PREFORM INFRARED RADIATIVE HEATING -RECENT RESULTS.

Serge Monteix[(*)], F. Schmidt[(*)], Y. Le Maoult[(1)(*)], G. Denis[(**)], M. Vigny[(**)]

[(*)]Ecole des Mines d'Albi-Carmaux Campus Jarlard, Route de Teillet, 81013 ALBI CT Cedex 09 (France)
[(**)] Perrier-Vittel M.T., BP 43 88805 Vittel Cedex (France),(1) : corresponding author.

ABSTRACT

The injection stretch-blow moulding process of thermoplastic bottles requires an heating step before forming. An amorphous preform is heated above the glass transition temperature (80°C for the P.E.T.) using an infrared oven. This step is fundamental in order to determine the thickness distribution along the preform height and then insure high quality bottles. Thus, the optimisation of the infrared oven is necessary. Various experiments have been conducted to characterise the heat source and the semi-transparent properties of the P.E.T. Measurements of air temperature inside the infrared oven and air cooling speed have been processed. These parameters have been implemented in a control volume software that simulates the heating step. The surface temperature distribution of the preform has been measured using an infrared camera. Comparisons between experimental and numerical results for a rectangular sheet and a rotating preform are presented.

1. Introduction

The injection stretch-blow moulding process of thermoplastic bottles requires a heating step before forming. An amorphous tube-shaped preform is heated above the glass transition temperature (80°C for the P.E.T.) using an infrared oven. As the P.E.T. conductivity is low (0.29 W/m.K), halogen lamps permit a rapid heating with a high flux intensity. In addition, a cooling fan is necessary in order to prevent P.E.T from thermal crystallisation that will induce non-amorphous preform. However, there are plenty of parameters such as number of lamps, distance between halogen lamps and preform, electrical power of the lamps, air cooling speed, reflectors, rotation speed, Therefore optimising infrared oven in order to design new plastic bottles is still a long and costly work. The main objective of this work was to develop a numerical software using control volume method that simulates the heating step of the preform. For that, we have to take into account influent parameters of the heating step such as halogen lamps, characterisation and P.E.T, spectral properties. In addition, we need to measure the preform temperature. We have used an 880 LW AGEMA infrared camera (connected to real time software) in order to measure external and internal preform surface temperature distribution, heat transfer coefficient along preform height. The air temperature surrounding the preform and inside the preform is measured using thermocouples.

1. Modelling of infrared PET preform heating

A 3D control-volume software, called PLASTIRAD, has been developed in order to compute heat transfer during the infrared-heating step. The preform (sheet or cylinder) is meshed using cubic or hexahedral elements so-called control volumes [1]. The temperature balance equation including radiative transfer (thermal power absorbed by the semitransparent P.E.T. preform and

radiated from halogen lamps) is integrated over each control volume and over the time from t to t+Δt (1):

$$\int_{\Delta t}\int_{\Omega_e} \rho\, c_p \frac{\partial T}{\partial t}\, d\Omega\, dt = -\int_{\Delta t}\int_{\Gamma_e} (\vec{q_c}.\vec{n})\, d\Gamma dt + \int_{\Delta t}\int_{\Gamma_e} (\vec{q_r}.\vec{n})\, d\Gamma dt \qquad (1)$$

Where Ω_e is the control-volume, q_c and q_r the Fourier's conductive and the radiative fluxes.The unknown temperatures are computed at the cell centres of the elements. The specific lamp geometry is also considered, taken into account from a view factor computation. The particular lamps used in the infrared oven are composed of a coiled tungsten filament (length : 300 mm), contained in a quartz tubular enclosure (diameter : 10 mm) filled with a neutral gas (Argon) and coated on its back with a ceramic reflector in order to increase the heat flux received by the product. In our model, we assume a constant filament temperature and then an uniform source temperature. Thus the amount of radiation, reaching each front elements of the irradiated preform, is performed with the contour method (2) using Stoke's theorem [2] :

$$F_{H\to p} = \frac{1}{2\pi S_H} \oint_{\Gamma_H}\oint_{\Gamma_{r_p}} \ln r.\vec{dr_H}.\vec{dr_{r_p}} \qquad (2)$$

where the subscripts H refers to the heater and p to the preform front element under consideration, r is the distance between two elemental linear elements, issued from the discretisation of the entire heater boundary Γ_H and Γr_p for each surface of control element's boundary reaching the irradiated preform's face. This contour method integration was chosen between different numerical view factor methods (Monte Carlo or geometrical method). This method allows a good accuracy with a very low computational time. An efficient numerical method based on Gaussian quadrature has been applied in order to perform the contour integration. The computation of the amount of incident radiation, for each surface element, is given in equation (3):

$$\Phi(r_p) = k_r F_{H\to r_p} \frac{S_H}{S_{r_p}} \int_{\Delta\lambda} \varepsilon_\lambda(T_{Fil})\pi L_\lambda{}^0(T_{Fil})\, d\lambda \qquad (3)$$

where ε_λ is the spectral tungsten emissivity, T_{fil} the filament temperature, $L_\lambda{}^0$ the blackbody intensity, λ a given wavelength between [0.2,10] μm and k_r the efficiency factor of the ceramic reflector. In a first approximation, internal radiative transfer is assumed to be mono-dimensional across the preform thickness. The PET bulk temperature ($\leq$400K) is very low in comparison to the source temperature (T_{fil} > 2000 K). So the assumption of cold material is convenient. This leads to express the transmitted flux across the thickness of the material, for an homogenous and amorphous PET, using the Beer-Lambert's law, if the coordinate y describe the thickness, we have, in a simple way, for the flux (4):

$$\Phi_\lambda(y) = \Phi_\lambda(y=0)e^{-k_\lambda y} \qquad (4)$$

where k_λ is the spectral absorption coefficient of our material.

Further details on this specific numerical model are given in [2].

2. Heat source characterisation : Filament and Quartz temperatures, efficiency of the reflector.

Spectral properties of these elements have already been measured in a previous work [2]. Using these data, the tungsten filament and quartz tube temperatures are calculated using a net radiation method [3] with (5):

$$\begin{cases} P - \varepsilon_{Fil}(T_{Fil}) S_{Fil} \sigma {T_{Fil}}^4 - 2\pi L_Q k_{Argon}(T^*) \dfrac{T_{Fil} - T_Q}{\ln(\dfrac{d_Q}{d_{Fil}})} = 0 \\ \alpha_Q(T_{Fil}) \varepsilon_{Fil}(T_{Fil}) S_{Fil} \sigma {T_{Fil}}^4 + 2\pi L_Q k_{Argon}(T^*) \dfrac{T_{Fil} - T_Q}{\ln(\dfrac{d_Q}{d_{Fil}})} - \varepsilon_Q S_Q \sigma {T_Q}^4 - h S_Q (T_Q - T_\infty) = 0 \end{cases} \quad (5)$$

where P is the electrical power of the lamps; the indices Fil and Q refer respectively to the filament and the quartz tube, T is the temperature, L is the length of the lamp, d the filament or the quartz tube diameter, ε, α the emissivity and absorptivity. T* is assumed to be equal to $\frac{T_{Fil} + T_Q}{2}$. We have simplified this model by computing directly total parameters instead of spectral ones (as emissivity and absorptivity) with polynomial functions depending on temperatures which is easier and saves time. The temperatures of the filament and the quartz tube are computed at steady state using a Newton-Raphson method. The results of this computation are shown on figure 1. Additional curves are plotted on the same graph, they are related to experimental mesurements : Colour temperature of the filament and temperature computed with a resistivity method. At the nominal power of 1 kW, we have found the following values :

table 1

Filament temperature (K)	Quartz temperature (K)
2360	730

As shown on figure 1, the discrepancy between the extremal curves is important : greater than 100 K around 2350 K. This fact is due to the lack of knowledge on the properties of this particular kind of tungsten (coiled filament). On the other hand, “colour” temperature remains difficult to measure at such level of power.To conclude, we have chosen the computed temperature as a “mean” temperature, lower and upper limits of the temperature, at 1 kW (see graph on figure 1), will be considered as the global uncertainty. Using experimental setup described in [2], the efficiency factor of the ceramic reflector has been measured :

$$k_r(\theta, T_r) = \frac{\Phi_r(\theta, T_r)}{\Phi_w(\theta, T_r)} \quad (6)$$

The indices r and w refer respectively to the lamp with a ceramic reflector and without reflector. θ the angle describe by a detector around the heater and T_r the temperature of the reflector. This value is obtained using a thermopile detector with a large spectral bandwidth [0.25,26μm] .

The output signal delivered by the thermopile is related to the flux emitted by the lamp, so the ratio of the two fluxes measured by the detector and introduced in (6) gives the efficiency of the coating. We have checked that this efficiency is unaffected by the variation of the temperature of the filament and that the emission of the lamp is quasi isotropic. Therefore, we have obtained :

$$k_r = 1.36 \pm 0.02$$

3.Characterisation of P.E.T. spectral properties

P.E.T. spectral properties measurements were performed using a 3-mm thick sheet. These sheets were processed by injection moulding in the same conditions than tubular preforms. Thermal analysis experiments were carried out in order to measure the sheets crystallinity. Samples of 10-15 mg weight were cut away from the thick sheet. The DSC experiments were performed on a Mettler calorimeter at a heating rate of 10°C/min. The average crystallinity value of these measurements was about 5 %, corresponding to an amorphous P.E.T, which confirms that diffusion of the radiation can be neglected. Then we have proceeded to P.E.T spectral properties measurements (transmitivity, reflectivity) using a Perkin-Elmer FT-IR spectrometer. The previous thick sheets were polished in order to obtain samples of 0.3-mm thickness, spectra are used as a database in the numerical simulation [5]. In addition, we have found that the polymer is opaque for wavelengths in the range of 8 to 12 μm with an integrated emissivity of 0.93. This bandwidth corresponds to the one of the infrared camera.

4. Experimental data

Figure 2 shows the experimental set-up developed on the basis of industrial infrared oven using in injection blow moulding machines. This device consists of six halogen lamps (Philips 1000 W-235 V SK15), monitored by power device. The preform is fixed on a rotating support to provide homogeneous hoop temperature. Behind the preform, there is a cooling fan controlled by a DC supply. A pneumatic system allows the preform displacement inside and outside the oven.

4.1 Measurement of the air temperature inside the oven

For the measurement of the air temperature inside the oven, J type thermocouples were used. They are connected to a Keithley recorder instrument. All thermocouples are shielded with aluminium adhesive tape. In order to place a thermocouple inside the preform, the top of this one is drilled (Figure 3).

4.2 Measurement of surface temperature distribution

The internal surface temperature measurement of a tubular preform is more tedious and necessitates to develop a specific process. First, we have to cut the preform in its longitudinal-section. Then, the two half-parts of the preform are sticking together using a conductive grease to insure joining during the heating time. All the lamps are set to the same temperature, coupled with the cooling fan, during 20 seconds. Then the rebuild preform exits from the oven in front of the camera. In order to make possible the internal surface temperature measurement, one half-parts is removed (immediately after preform recovering or after a characteristic inversion time).

This particular method and the results associated (Infrared thermograms) have been presented in reference [5].

4.3 Measurement of air forced convection heat transfer coefficient

In this section, we want to determine the air forced convection heat transfer coefficient, generated by the cooling fan along the preform height. Two different methods are developed and compared. The first one consists in measuring air-cooling speed using a hot wire anemometer (Ans Snelco). The calculated Reynolds numbers deduced from these data are in the range between 4000 and 10000 that is to say a turbulent flow. Then, we identify from the literature [3] different classical relationships that are suitable for a cylinder in cross flow, i.e. $\mathrm{Nu} = \mathrm{f}(\mathrm{Re}, \mathrm{Pr})$. The second method is based upon the preform surface temperature measured by the infrared camera in presence of cooling flow. The following specific experimental procedure has to be observed in order to compute the heat transfer coefficient: first, a 20 seconds heating time coupled with cooling; then turn off heating and cooling in order to insure an uniform temperature throughout the preform thickness; then restart the cooling fan. Thus, the last step of the procedure allows solving analytically the energy balance integrated over the thickness if we assume that the main part of the preform is a hollow tube. For a given height, the relationship for the heat transfer coefficient h yields:

$$h = -\frac{\rho\, Cp\left(\frac{d\bar{T}}{dt}\right)_{t=0}}{\left(\bar{T}_o - T_\infty\right)} \frac{Re^2 - Ri^2}{Re} \qquad (7)$$

Where $\bar{T}$ is the thickness-average temperature, C_p the P.E.T heat capacity, ρ the P.E.T specific mass, $\bar{T}_\infty$ the thickness-average ambient temperature, R_e and R_i are respectively the external and internal preform radii. R_i is computed using the depth penetration throughout the preform over a characteristic time t, for which we have sufficient temperature data to calculate the initial slope $\left(\frac{d\bar{T}}{dt}\right)_{t=0}$ of the temperature-time plot (figures 4).

$$Ri = Re - e = Re - 2\sqrt{\alpha\, \Delta t}\,\beta \qquad (8)$$

Where α is the P.E.T diffusivity and β the argument of the erf function, computing assuming the surface temperature has decreased of 90% at the depth thickness. In figures 4, we present a comparison between the heat coefficient measured using both methods. The agreement between the two different methods is fair. It permits to calculate an average air cooling heat transfer coefficient of 45 ± 5 W/m^2.K. The same experiment has been conducted on different industrial ovens and the values of h are in the range [35,60] W/m^2.K which is very close to our laboratory results.

5. Numerical simulation

We performed simulation of the heating step for a P.E.T sheet and a tubular preform, taking into account processes parameters introduced previously. The values of the main parameters are summarised in the tables 2 and 3 below, results are presented on figures 5,6 and 7:

5-1)PET sheet -dimensions : 180*100*3 mm / lateral faces are insulated.

table 2

Heating time (s)	Cooling time (s)	Number of lamps	Dist.lamps-preform /mm	h (W/m^2.K)	Lamps Temp. (K)	Rotation speed (r s^{-1})
65	-	1	40	8 (natural)	2360	-

5-2) Tubular Preform (diameter : 25 mm,height : 100 mm, thickness : 3 mm)

table 3

Heating time (s)	Cooling time (s)	Number of lamps	Dist. lamps-preform /mm	h ($W/m^2 \cdot K$)	Lamps Temp. (K)	Rotation Speed ($r\ s^{-1}$)
20	20	6	20	45	2360	1.2

Discussion : The comparison on figure 5 shows a relative error of 5 % on the peak temperature and 10 % on the boundary on the sheet which appears as a 3D effect related to the transmission of the radiative flux inside the material. Figures 6 shows simulated surface temperatures distribution on a tubular preform. More important is the Figure 7 that shows a discrepancy of 17 °C between numerical computation and experimental data (versus time). As we have investigated this problem, we can say that, the model, doesn't take into account the reflectivity (in the oven) of the cooling fan nozzle, composed of a metallic plate with several slits, nor does it take into account the flux reflected by the preform from the lamps. This first effect has been evaluated thru measurements. Its influence is close to 3°C in the final apparent temperature indicated by the camera. In the same way, the reflectivity coefficient deduced from spectrometry measurements : 7 % for the 8-12 μm spectral band, leads to a 4°C error on the measurement (computed from a thermal image difference). At last, the total error is equal to 7°C and the true measured temperature should be equal to 110°C. Therefore, the real relative error between experimental results and computations as shown on figure 7 will be close to 10%.

Conclusion

Numerical simulations of P.E.T preform heating stage have been performed by using Characterisations of halogen lamps and P.E.T spectral properties. All the measured parameters have been included in the numerical model. The agreement between numerical simulations and experimental data is fair considering the simple model used for absorption (Beer-Lambert law). The infrared camera appears as a powerful device to make quantitative temperature measurements on the preform and to assess the numerical simulations. Future developments will include new techniques in measurements as temperatures in the preform thickness and improvements in the radiative transfer computations used in the model (rotation of the preform).

Acknowledgements : Perrier-Vittel Company supports this work. Special thanks go to J-P. Arcens for his help on the experiments.

Reference

[1] Patankar S.V., "Numerical Heat Transfer and Fluid Flow ", Ed. Mc Graw Hill, New-York, 1980

[2] Rammohan R., " Efficient Evaluation of Diffuse View Factors For Radiation", Int. Journal . Heat and Mass Transfer, Vol 39,N°6 p1281-1286-1996.

[3] Monteix S., Schmidt F., Le Maoult Y. "Modélisation du chauffage infrarouge de plaques en P.E.T", IV^{e} Colloque Interuniversitaire Franco-Québecois, "Thermique des systèmes à température modérée", Montréal –Québec-1999.

[4] Petterson M., "Heat Transfer and Energy Efficiency in Infrared Papers Dryers", Ph. D. Thesis, Lund University, Sweden-1999.

[5] Monteix S., Schmidt F., Le Maoult Y. "Experimental study and Numerical Simulation of Sheet and Tubular preform Infrared Heating", QIRT 2000, Eurotherm Seminar N°64-Reims-France.

[6] Incropera F. De Witt D.P.," Fundamentals of heat and mass transfer", Third Ed. 1990

Figures

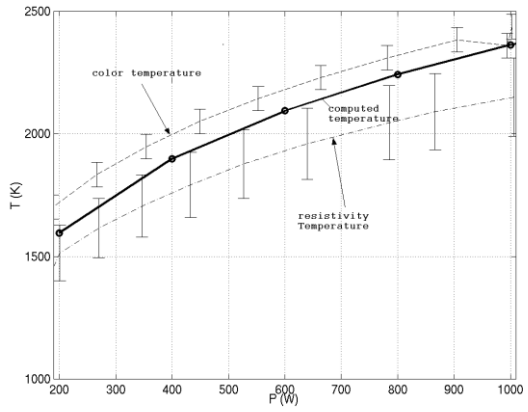

figure 1 : Filament temperature versus electrical power

figure 2 :Experimental setup, the infrared oven

figure 3 : Thermocouples oven' instrumentation (inside the tubular preform and air temperature)

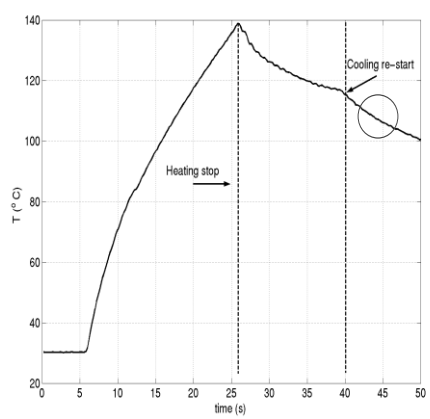

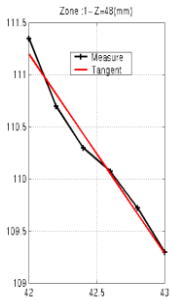

figures 4 : Surface temperature versus time (cooling) infrared measurements

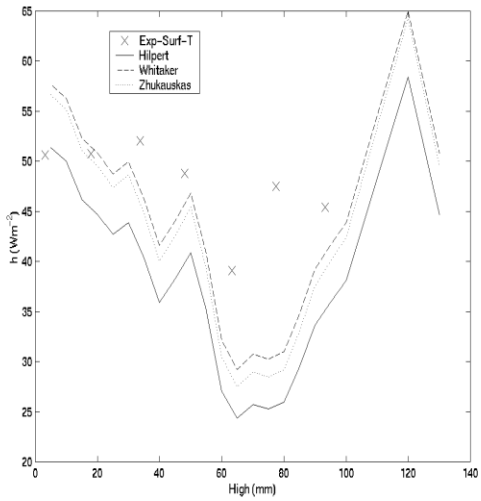

Forced convection coefficients (along the preform height)

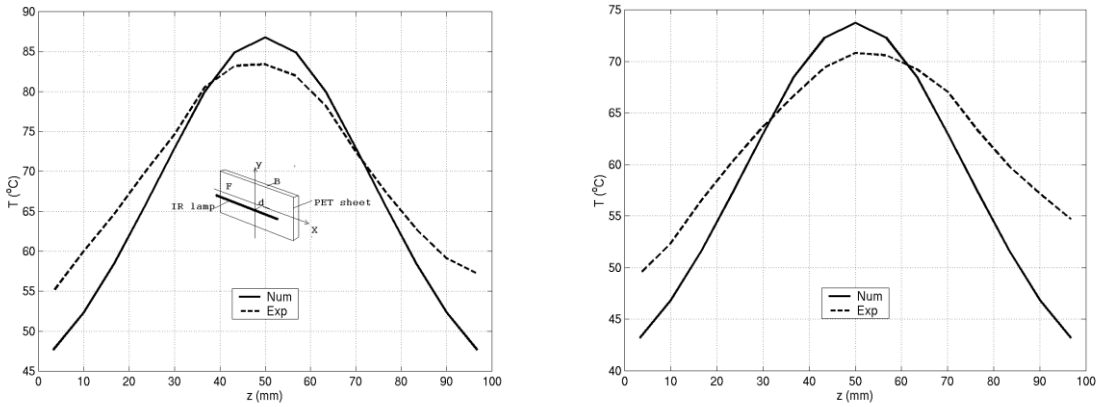

figures 5 : comparison, for a PET sheet, between experimental data (IR Thermography), and numerical computation. Y- profiles : on the left the Front face (in front of the lamp), on the right side , the Back face (parameters list : table 2)

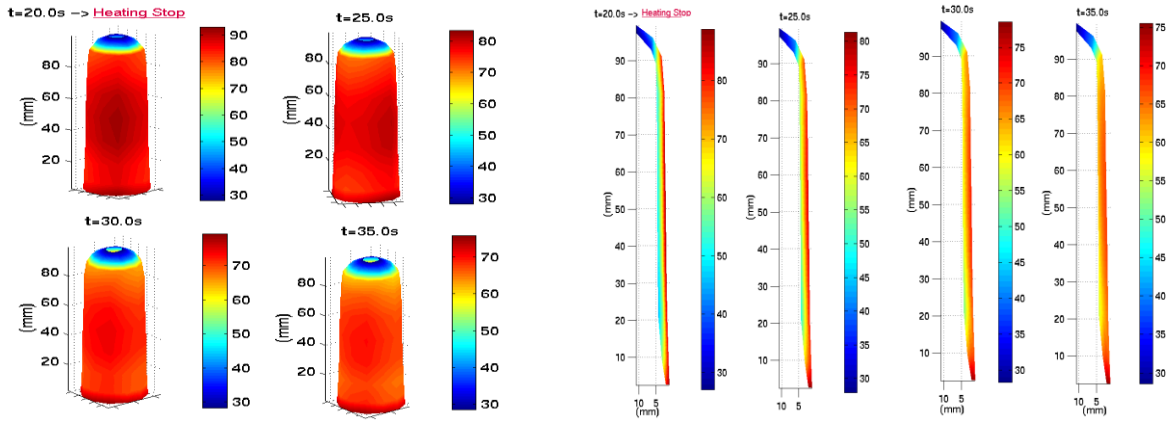

figures 6 : numerical simulation with parameters listed in table 3 (heating and cooling)

Numerical simulation of preform temperature across the thicknes

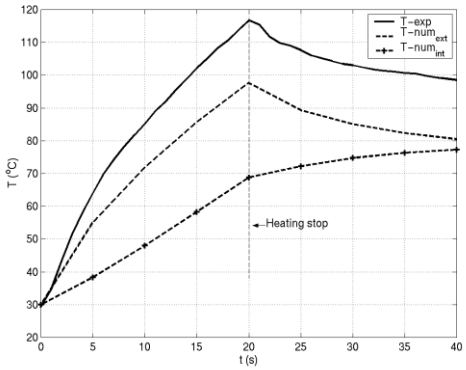

figure 7 :comparison between experimental (temporal marker)and numerical temperature versus time for a tubular preform (front and internal faces)